Substitution at Residue 214 of Human Thymidylate Synthase Alters Nucleotide Binding and Isomerization of Ligand−Protein Complexes†

David J. Steadman,‡ H. Trent Spencer,§ R. Bruce Dunlap,‡ and Sondra H. Berger*,‖

Departments of Chemistry and Biochemistry, Basic Pharmaceutical Sciences, and Biological Sciences, University of South Carolina, Columbia, South Carolina 29208

Received December 10, 1998; Revised Manuscript Received February 22, 1999

ABSTRACT: Based on crystal structures of bacterial thymidylate synthases (TS), a glutamine corresponding to residue 214 in human TS (hTS) is located in a region that is postulated to be critical for conformational changes that occur upon ligand binding. Previous steady-state kinetic studies indicated that replacement of glutamine at position 214 (Gln214) of hTS by other residues results in a decrease in nucleotide binding and catalysis, with only minor effects on folate binding (D. J. Steadman et al. (1998) *Biochemistry 37*, 7089−7095). The data suggested that Gln214 maintains the enzyme in a conformation that facilitates nucleotide binding. In the present study, transient-state kinetic analysis was utilized to determine rate constants that govern specific steps along the catalytic pathway of hTS, which provides the first detailed kinetic mechanism for hTS. Analysis of the reaction mechanisms of mutant TSs revealed that substitution at position 214 significantly affects nucleotide binding and the rate of chemical conversion of bound substrates to products, which is consistent with the results of steady-state kinetic analysis. Furthermore, it is shown that substitution at position 214 affects the rate of isomerization, presumably from an open to a closed form of the enzyme−substrate complex. Although the affinity of the initial binding of CH_2H_4folate is not substantially affected, K_{iso}, the ratio of the forward rate of isomerization (k_{iso}) to the reverse rate of isomerization ($k_{r,iso}$), is 2−6-fold lower for the mutants at position 214 compared to Q214, with the greatest effects on k_{iso}. In addition, the binding of the folate analogue, CB3717, to dUMP binary complexes of mutant enzymes was characterized by a slow isomerization phase that was not detected in binding studies utilizing wild-type hTS. The data are consistent with the hypothesis that Gln214 is located at a structurally critical region of the enzyme.

Thymidylate synthase (TS[1]; EC 2.1.1.45) catalyzes the reductive methylation of dUMP using the cofactor 5,10-methylenetetrahydrofolate (CH_2H_4folate) to form TMP and dihydrofolate (H_2folate). The TS reaction is initiated by nucleophilic addition at C-6 of dUMP by the catalytic cysteine (Figure 1). The activated enolate intermediate forms a covalent ternary complex with CH_2H_4folate. Following removal of the proton at C-5 of the pyrimidine ring, an exocyclic methylene is formed with elimination of tetrahydrofolate (H_4folate). The exocyclic methylene is reduced by hydride transfer from H_4folate, which is oxidized to H_2folate.

Since TS provides the only *de novo* source of TMP, it has long been a target of chemotherapy. The fluoropyrimidine drugs, 5-fluorouracil and 5-fluorodeoxyuridine (FdUrd), are antimetabolites that have been utilized extensively to inhibit TMP production. The fluoropyrimidines are metabolized to FdUMP, a fluorinated analogue of dUMP. Upon binding of FdUMP and CH_2H_4folate to TS, an inhibitory ternary

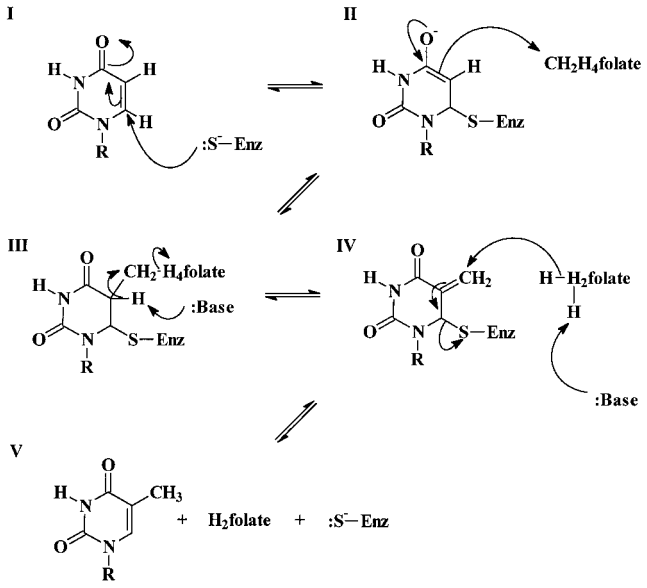

FIGURE 1: Key steps of the chemical mechanism of TS. The figure is adapted from Carreras and Santi, 1995 (*3*).

† Research supported by NIH Grants CA 64566 and CA 76560.

* To whom correspondence should be addressed: Department of Basic Pharmaceutical Sciences, University of South Carolina, 700 Sumter Street, Columbia, SC 29208; E-mail: berger@pharm.sc.edu.

‡ Departments of Chemistry and Biochemistry.

§ Department of Biological Sciences.

‖ Department of Basic Pharmaceutical Sciences.

[1] Abbreviations: TS, thymidylate synthase (EC 2.1.1.45); hTS, human TS; ecTS, *Escherichia coli* TS; lcTS, *Lactobacillus casei* TS; CH_2H_4folate, (6*R*)-5,10-methylene-5,6,7,8-tetrahydrofolate; H_2folate, 7,8-dihydrofolate; dUMP, 2′-deoxyuridine-5′-monophosphate; TMP, thymidine-5′-monophosphate; FdUMP, 5-fluoro-2′-deoxyuridine-5′-monophosphate; CB3717, 10-propargyl-5,8-dideazafolate; AG337, 3,4-dihydro-2-amino-6-methyl-4-oxo-5-(4-pyridylthio)-quinazoline dihydrochloride; SDS−PAGE, sodium dodecyl sulfate−polyacrylamide gel electrophoresis.

10.1021/bi982910n CCC: $18.00
Published on Web 04/09/1999

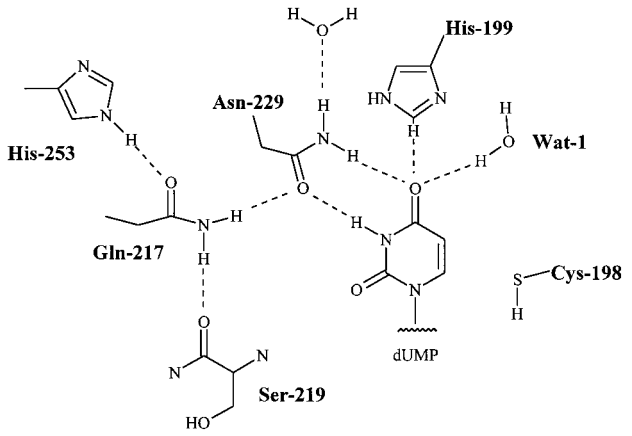

FIGURE 2: Proposed role of Gln217 in lcTS. Diagram showing the proposed hydrogen bond network of highly conserved residues at the active site, including Gln217 (corresponding to Gln214, hTS), and 3-NH and 4-O of dUMP. The figure is adapted from Finer-Moore et al. (*10*).

complex is formed in which the enzyme is locked into an inactive state. More recently, inhibitors, such as CB3717 and AG337, have been developed that are analogues of CH_2H_4folate. These agents bind tightly to TS, inhibiting the enzyme at nanomolar and even subnanomolar concentrations (*1*, *2*).

Due to the clinical importance of TS, the structure and catalytic mechanism of wild-type and mutant TSs from many sources have been examined (*3*). In recent studies of human TS (hTS), it was shown that replacement of glutamine at position 214 of hTS decreases the affinity of the enzyme for FdUMP in the presence of CH_2H_4folate in vitro (*4*). Studies of a mutant TS in which glutamine is replaced by glutamate revealed that the decrease in affinity of the mutant enzyme for FdUMP is associated with resistance to FdUrd (*5*). Furthermore, substitution of glutamine at position 214 by arginine was associated with resistance to the antifolate, AG337 (*6*). Crystallographic studies indicated that glutamine at this relative position in *Escherichia coli* TS (Gln165) is located within one of three β-bulges that collectively form a β-kink (*7*). This β-kink is thought to be critical for conformational changes that occur upon ligand binding, with the major effect being induced by the folate ligand (*8*). Upon ligand binding, there is a shift of residues toward the active site (*8*, *9*) ranging from 0.3 Å for residues near the β-bulge to 4 Å for the C-terminal residues (*8*).

Crystallographic studies suggested that Gln217 of *Lactobacillus casei* TS (the relative position of Gln214 in hTS) interacts with bound nucleotide through a hydrogen bonding network with adjacent residues (ref *10*; Figure 2). Steady-state kinetic analysis indicated that mutations at position 214 of hTS negatively affect ligand binding and catalysis (*4*). The presence of a charged residue (aspartate, glutamate, lysine, or arginine) or a large side chain volume (leucine, phenylalanine, or tryptophan) significantly reduced or eliminated catalysis. The major effect of substitution at position 214 was on K_m for nucleotide binding, with only minor effects on CH_2H_4folate binding. From these studies, it was proposed that glutamine at position 214 maintains the enzyme in a conformation that facilitates nucleotide binding.

To obtain additional information on the effect of substitution at position 214 of hTS, transient-state kinetic analysis was utilized to determine kinetic and thermodynamic constants for nucleotide and folate binding to wild-type hTS (Q214). The data provided herein represent the first detailed description of the reaction mechanism of hTS. In addition, the reaction mechanisms of representative mutant enzymes that are catalytically active were analyzed and compared to that of the wild-type enzyme. The data indicate that substitution at position 214 significantly affects nucleotide binding and the rate of isomerization that occurs after binding of the folate ligand to an enzyme−dUMP binary complex.

EXPERIMENTAL PROCEDURES

Materials. Nucleotides, salts, 2-mercaptoethanol (2-ME), glycerol, and folic acid were obtained from Sigma (St. Louis, MO). (6*S*)-5,6,7,8-Tetrahydrofolic acid was prepared from folic acid and converted to (6*R*)-5,10-CH_2H_4folate as described previously (*11*). CB3717 was generously provided by Zeneca Pharmaceuticals (Macclesfield, U.K.).

Purification of Wild-Type and Mutant Enzymes. Enzymes were purified as described previously with modification (*4*). The size exclusion chromatographic step was replaced with Q-Sepharose (Pharmacia, Piscataway, NJ) ion-exchange chromatography. TS was eluted from the Q-Sepharose column with a linear gradient of 0.2−0.4 M KCl. TS purity was demonstrated by 12% SDS−PAGE. Purified TS was stored at −20 °C in buffer A (50 mM Tris base, 1 mM EDTA, and 14 mM 2-ME; pH 7.4) containing 15% glycerol.

Stopped-Flow Measurements. Kinetic data describing the interaction of ligands with Q214 and mutant enzymes were obtained using an Applied Photophysics Hi-Tech SX.18MV stopped-flow fluorimeter/spectrometer (Applied Photophysics, United Kingdom). Transient kinetic data were obtained with an excitation wavelength of 295 nm by monitoring intrinsic enzyme fluorescence above 330 nm. Experiments were conducted using enzyme and ligands diluted in buffer A. Measurements were performed at 20 °C, and temperature was maintained by a Fisher refrigerated model 900 circulating water bath (Fisher Scientific, Norcross, GA). Final enzyme concentrations were 2 μM unless otherwise noted. Data were collected and analyzed online using SpectraKinetic Workstation software (version 4.24, Applied Photophysics, U.K.) or Kaleidagraph (version 3.0, Abelbeck Software, Reading, PA). Fluorescence measurements used to calculate pseudo-first-order rate constants (k_{obs}) were an average of at least 4 traces. Experiments were repeated at least two separate times, and reported values are within an experimental error of 10%.

Determination of Kinetic and Thermodynamic Constants for Nucleotide Binding to Wild-Type and Mutant Enzymes. Kinetic and thermodynamic parameters for binding of nucleotides to wild-type and mutant enzymes were determined by titrating enzymes with various concentrations of dUMP, FdUMP, or TMP. Data were collected over 20 or 50 ms time periods. Final concentrations of dUMP, FdUMP, and TMP were 5−200, 10−250, and 5−250 μM, respectively.

Determination of Kinetic and Thermodynamic Constants for CH_2H_4Folate Binding to Wild-Type or Mutant Enzymes in the Presence of dUMP. Kinetic and thermodynamic parameters for CH_2H_4folate were measured by titrating the binary complex of hTS and dUMP with various concentrations of CH_2H_4folate. Data were collected over a 1 s time

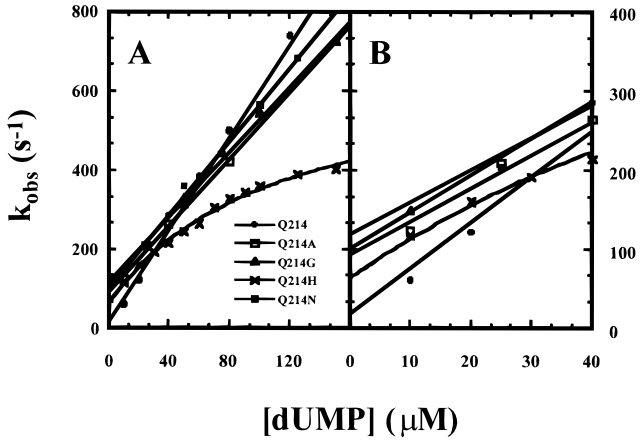

FIGURE 3: The dependence of k_{obs} on dUMP concentration. The dependence of k_{obs} on dUMP concentration was determined at dUMP concentrations of 0−150 μM, as described in Experimental Procedures.

Scheme 1

$$\text{hTS + N} \underset{k_{off}}{\overset{k_{on}}{\rightleftharpoons}} \text{hTS.N}$$

period. The concentration range of CH_2H_4folate was 5−250 μM. The final concentration of dUMP was 0.50 mM for Q214, Q214A, and Q214N and 1.0 mM for Q214G and Q214H.

Determination of the Kinetics of CB3717 Binding to Wild-Type or Mutant Enzymes in the Presence of dUMP. The kinetics of CB3717 binding were measured by titrating the binary complex of hTS (1 μM final concentration) and dUMP (0.50 or 1.0 mM final concentration) with final concentrations of CB3717 ranging from 2 to 6 μM. Data were collected over 20 or 50 ms time periods.

*Determination of Activation Energy (E_a) for Wild-Type and Mutant Enzymes.*The dependence of k_{cat} on temperature was used to calculate E_a for Q214 and mutant enzymes. Enzyme activity was measured spectrophotometrically by monitoring the absorbance change accompanying the conversion of CH_2H_4folate to H_2folate (*12*). Measurements were performed at pH 7.4 in Morrison buffer (*13*). Velocity was measured at temperatures ranging from 20 to 37 °C. Temperature was maintained by a temperature-controlled cell holder attached to a Shimadzu 1601 spectrophotometer (Shimadzu Corp., Columbia, MD). Rates were measured using 50 nM purified TS, 150 μM dUMP, and 500 μM CH_2H_4folate.

RESULTS

Determination of Kinetic and Thermodynamic Constants for Nucleotide Binding to hTS. Fluorescence data were analyzed by using single-exponential (Q214, Q214A, and Q214N) or double-exponential (Q214G) curve fits. The dependence of k_{obs} on nucleotide concentration was linear for all enzymes except Q214H, which was hyperbolic (Figure 3). Kinetic and thermodynamic constants for nucleotide binding to Q214, Q214A, Q214G, and Q214N were determined as previously described (*14*) using the model of nucleotide binding shown in Scheme 1. Constants for nucleotide binding to Q214H were determined using a model described by Mittelstadt and Schimerlick (*15*) for nucleotide binding to wild-type *L. casei* TS (Scheme 2). The model is a two-step mechanism with an initial, weak association between Q214H and nucleotide, followed by an equilibrium isomerization that increases the affinity of the enzyme for the nucleotide. With the use of this model, the initial binding constant is described by K_{int}, the forward and reverse rates of isomerization are represented by k_{+1} and k_{-1}, respectively, and the overall binding affinity following isomerization is K_{ov}.

Scheme 2

$$\text{hTS + N} \underset{}{\overset{K_{int}}{\rightleftharpoons}} \text{hTS.N} \underset{k_{-1}}{\overset{k_{+1}}{\rightleftharpoons}} \text{hTS.N*}$$

Table 1: Kinetic and Thermodynamic Constants for TMP Binding to Q214 and Mutant Enzymes

enzyme	k_{on} (s^{-1})	k_{off} (s^{-1})	K_d[a] (μM)
Q214	3.8	35	9.2
Q214A	2.3	196	85
Q214G	2.6	226	87
Q214N	2.0	271	140

[a] Determined from the ratio of k_{off}/k_{on}.

Table 2: Kinetic and Thermodynamic Parameters for Nucleotide Binding to Q214H

nucleotide	K_{int} (μM)	k_{+1} (s^{-1})	k_{-1} (s^{-1})	K_{ov}[a] (μM)
dUMP	123	628	72	13
TMP	140	585	132	25
FdUMP	75	499	92	12

[a] Calculated using the expression $K_{ov} = K_{int}K_1/(1 + K_1)$, where $K_1 = k_{-1}/k_{+1}$.

Kinetic and thermodynamic constants for binding of dUMP and FdUMP to Q214, Q214A, Q214G, and Q214N were published previously (*4*). Kinetic and thermodynamic constants for the binding of TMP to wild-type and mutant enzymes are shown in Table 1. As observed with dUMP and FdUMP binding, the k_{on} values for TMP were similar for Q214, Q214A, Q214G, and Q214N, while k_{off}s were significantly increased for the 3 mutant enzymes (*4*). The values of k_{off} for dUMP and FdUMP of the 3 mutant proteins were increased by 4−8-fold and 9−13-fold, respectively, relative to Q214 (*4*). As shown in Table 1, k_{off}s for TMP of the 3 mutant proteins were increased by 6−8-fold, relative to Q214. As shown in Table 2, the values of K_{int} were similar for the binding of all nucleotides to Q214H. The isomerization following initial nucleotide binding increased the affinity of Q214H for the nucleotides by 6−9-fold.

Determination of Kinetic and Thermodynamic Constants for CH_2H_4Folate Binding to the Binary Complex of hTS·dUMP. The time courses of fluorescence quenching were analyzed as previously described (*14*) using a single-exponential curve with a steady-state parameter, which accounts for product formation. The model used to describe CH_2H_4folate binding to hTS·dUMP is shown in Scheme 3. When hTS was mixed with substrates, a burst in fluorescence (k_{burst}) at 340 nm was observed. The dependence of k_{burst} on CH_2H_4folate concentration was hyperbolic for Q214 and the mutant enzymes. Kinetic and thermodynamic constants were determined using the following relationship: $k_{burst} = k_{iso}[L]/(L + K_d) + k_{r,iso} + k_{chem}$. The kinetic and thermodynamic parameters for binding of CH_2H_4folate to the binary complex

Scheme 3

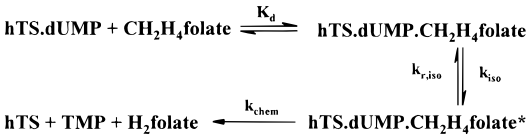

Scheme 4

Table 3: Kinetic and Thermodynamic Constants for CH_2H_4Folate Binding to Q214 and Mutant Enzymes in the Presence of dUMP

enzyme	K_d (μM) CH_2H_4folate	k_{iso} (s^{-1})	$k_{r,iso}$ (s^{-1})	K_{iso}[a]	k_{chem}[b] (s^{-1})
Q214	89	49	1.6	31	1.1
Q214A	105	15	2.8	5.4	0.7
Q214G	118	9.6	1.3	7.4	0.6
Q214H	141	34	2.7	13	0.9
Q214N	110	28	4.8	5.9	0.7

[a] Determined from the ratio of k_{iso} to $k_{r,iso}$. [b] Calculated using the expression $k_{cat} = k_{chem}(1 + k_{r,iso}/k_{iso})$, assuming a k_{cat} of 1.0 s^{-1} at 20 °C.

Table 4: Rates of Association and Isomerization for CB3717 Binding to Q214 and Mutant Enzymes in the Presence of dUMP

enzyme	k_{on} (s^{-1})	$k_{iso} + k_{r,iso}$ (s^{-1})
Q214	147	nd[a]
Q214A	153	32
Q214G	142	26
Q214H	129	45
Q214N	138	37

[a] None detected.

of hTS·dUMP are listed in Table 3. The K_d values for CH_2H_4folate binding were only slightly increased for the mutant enzymes relative to Q214. However, compared with Q214, the values of k_{iso} were decreased for the mutants by 1.5−6-fold. The values of $k_{r,iso}$ were increased by 2−3-fold for Q214A, Q214N, and Q214H relative to Q214, while $k_{r,iso}$ for Q214G was only slightly decreased compared to Q214. Relative to Q214, each mutant enzyme exhibited a decrease in k_{chem}.

Determination of the Kinetics of CB3717 Binding to the Binary Complex of hTS·dUMP. Intrinsic enzyme fluorescence was quenched upon CB3717 binding to hTS in the presence of dUMP. Time courses of fluorescence quenching were fit to either $F_{(t)} = \Delta F\exp^{(k_{obs}t)} + F_{equ}$ or $F_{(t)} = \Delta F_1\exp^{(k_{obs}1t)} + \Delta F_2\exp^{(k_{obs}2t)} + F_{equ}$, where $F_{(t)}$ is the fluorescence at time t, ΔF is the amplitude of the fluorescence change, k_{obs} is the rate constant for each process, and F_{equ} is the fluorescence at equilibrium. The model used to describe CB3717 binding to hTS·dUMP is shown in Scheme 4. The values of k_{obs} were linearly dependent on CB3717 concentration, and the data extrapolated to near zero for all of the enzymes examined. Because CB3717 is a tight-binding inhibitor of TS, the value of k_{off} was too small for accurate determination. The rate constant governing the association (k_{on}) of CB3717 binding to Q214·dUMP was 147 s^{-1}, and similar rates were observed for each mutant enzyme (Table 4). A slow phase of fluorescence change, proposed to represent $k_{iso} + k_{r,iso}$, was not present for CB3717 binding to Q214·dUMP; however a distinct slow phase was present for CB3717 binding to binary complexes of dUMP and mutant enzymes (Table 4).

Table 5: Activation Energies (E_a) for Q214 and Mutant Enzymes

enzyme	E_a[a] (kJ/mol)	enzyme	E_a[a] (kJ/mol)
Q214	43 ± 3	Q214H	48 ± 4
Q214A	49 ± 2	Q214N	48 ± 2
Q214G	54 ± 4		

[a] Determined from the slopes of Arrhenius plots.

Determination of Activation Energy (E_a) for Wild-Type and Mutant Enzymes. The dependence of k_{cat} on temperature was determined for Q214 and mutant enzymes. The data were plotted as the natural logarithm of k_{cat} ($\ln k_{cat}$) versus inverse temperature in degrees Kelvin (K), and E_a was calculated from the Arrhenius equation: $\ln k_{cat} = \ln A - E_a/RT$. Activation energies for Q214 and the mutant enzymes are listed in Table 5. The value of E_a for Q214 was 43 kJ/mol. The mutant enzymes showed a 10−30% increase in the value of E_a compared to Q214.

DISCUSSION

Crystallographic studies of ecTS revealed that glutamine at the position corresponding to 214 in hTS is located at a β-bulge that is postulated to be important for ligand-induced conformational changes (*8*). Furthermore, studies of lcTS indicated that the glutamine residue corresponding to position 214 in hTS interacts with the nucleotide through a hydrogen bonding network with adjacent residues (*10*). Steady-state kinetic and equilibrium binding studies have also suggested that Gln214 is important for nucleotide binding as well as catalysis (*4*). From these studies, it was proposed that Gln214 is involved in maintaining a conformation that facilitates nucleotide binding.

To further analyze the effects of mutation at position 214, stopped-flow fluorescence spectroscopy was utilized to study the transient kinetics of ligand binding and isomerization of Q214 and mutant enzymes. These studies were consistent with previous steady-state results, which suggested that substitutions at this residue exert significant effects on nucleotide binding. The affinities of the mutant enzymes for all nucleotides examined were decreased, mainly due to an increased rate of dissociation. Interestingly, a nonlinear dependence of k_{obs} on nucleotide concentration was observed for Q214H (Figure 3), suggesting that an enzyme isomerization occurs that significantly increases the affinity of the enzyme for nucleotide (Table 2). Alternatively, the hyperbolic dependence of k_{obs} on dUMP concentration may arise from artifactual effects that result from either protein instability or differences in ligand preparation. This latter possibility is unlikely since the stability of Q214H was not substantially different from other Q214 mutants and the same ligand preparation was utilized in all investigations.

The dependence of k_{obs} on nucleotide concentration for Q214G was linear, but a concentration-independent slow phase was observed. Because this phase was not observed with other Q214 variants, it likely represents a process unique to this variant, in which an isomerization occurs following initial binding of the nucleotide that does not appear to affect the affinity of the enzyme for nucleotide. The isomerization events that were observed in Q214G and Q214H are most likely due to differences in side chain volume, which is

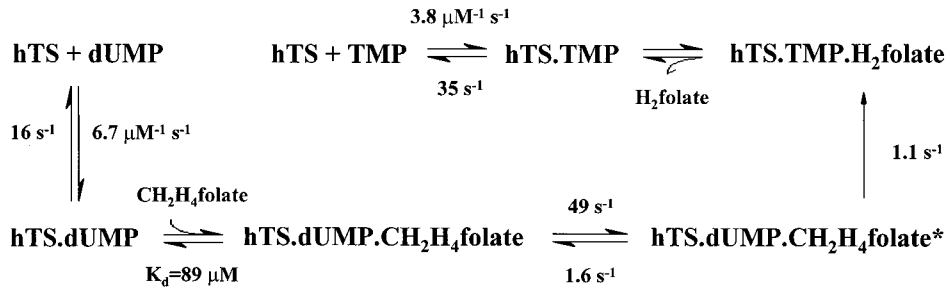

FIGURE 4: Kinetic scheme for the productive pathway of TMP synthesis for wild-type hTS. Kinetic and thermodynamic constants for TMP synthesis were determined as described in Experimental Procedures.

significantly smaller with glycine and larger with histidine, compared to glutamine.

Substitutions at 214 were shown to affect the rates of interconversion from open to closed forms of the enzyme−substrate complex. The K_{iso} data indicated that the conformation of Q214 is shifted toward a closed state on binding of dUMP and CH_2H_4folate, while that of the mutant enzymes is shifted toward an open state (Table 3). The major factor contributing to the observed differences in K_{iso} was the value of k_{iso}. An excellent correlation was observed between k_{iso} and the side chain volume for the mutant enzymes, with Q214G and Q214H exhibiting the slowest and fastest rates, respectively. An inverse relationship was observed between k_{iso} and the K_d for nucleotide binding. On the basis of crystal structures of ecTS (*17*), it was suggested that folate binding contributes significantly to the energy required for enzyme isomerization. In hTS, substitutions at 214 had little effect on the K_d for folate binding, yet the k_{iso} for isomerization was significantly different between the wild-type and mutant TSs. This suggests that the energy of isomerization is a result of productive binding of both substrates.

In previous studies, the forward and reverse rates of isomerization were determined for ecTS (*14*). Comparison of the values for hTS and ecTS revealed that k_{iso} is similar; however, $k_{r,iso}$ for hTS is decreased by 6-fold compared to that for ecTS. Crystallographic studies of unliganded hTS indicated that a loop containing the catalytic cysteine (Cys195) is reoriented 180° relative to its position in ecTS and lcTS (*16*). If this structure reflects the solution structure, hTS must undergo a unique conformational change relative to bacterial TSs in order to catalyze the enzymatic reaction. Perhaps favorable interactions are established upon the shift in conformation of the active site loop, which maintains hTS in the closed conformation.

Conformational effects due to substitution at position 214 were also observed with CB3717 binding in the presence of dUMP (Table 4). Previous transient-state kinetic studies of CB3717 binding to ecTS·dUMP revealed the existence of a concentration-independent slow phase with a maximum rate of 40 s^{-1} (*14*). On the basis of studies with mutant enzymes, it was suggested that the slow phase represents a conformational change in the enzyme, rather than covalent bond formation between dUMP and the active site cysteine. This slow phase was not observed in studies of CB3717 binding to Q214·dUMP. However, a definite concentration-independent slow phase was detected in studies of the binding of CB3717 to binary complexes of mutant enzymes. It is possible that significant reorientation must occur within the mutant enzymes, which is manifested as a pronounced slow phase, a process that is not detected with the wild-type enzyme. The absence of this phase for Q214 indicates that conformational differences exist not only between wild-type and mutant hTSs, but also between human and bacterial enzymes upon binding of CB3717. This is consistent with the differences in k_{iso} between hTS and ecTS that were observed after binding of the folate substrate.

An additional effect of substitution at position 214 was an increase in E_a for the mutant enzymes relative to Q214. One interpretation of the data is that the binding energy that contributes to the isomerization step of the mutant enzymes is not sufficient to induce the enzyme transition state complementarity of the wild-type enzyme. Alternatively, an increase in E_a may be due to a loss in a hydrogen bond network that stabilizes the transition state. For all enzymes, the values of E_a were inversely related to k_{chem}, indicating that the increased energy of activation for the mutants is related to the chemical steps after isomerization. In addition, k_{chem} values correlated well with the observed values of k_{cat} at 20 °C (data not shown). Previous studies of E_a of wild-type hTS purified from a human colon tumor cell line (HCT116/200-10) revealed that enzyme activity decreased above 35 °C (*18*). No decrease in activity was observed at temperatures up to 37 °C with the recombinant enzymes. This suggests that hTS isolated from the human cell line is more temperature-sensitive than recombinant hTS. The basis for the difference in thermal stability of the native and recombinant hTS is unknown.

Collectively, the data indicate that substitutions at position 214 affect nucleotide binding, ligand-induced isomerization, and rate of chemical catalysis. Previous investigations suggested that a loss of hydrogen bonding interactions at position 214 is not solely associated with the observed differences in nucleotide binding (*4*). Consistent with this interpretation, Q214A and Q214N exhibited no significant differences in either nucleotide binding or k_{chem} in transient kinetic studies. It is possible that hydrogen bonding interactions are maintained by compensatory changes in the position of water molecules, as has been observed in X-ray structures of other mutant enzymes (*19*, *20*). Thus, a water molecule could substitute for an amide group in the Q214A and Q214G mutants to maintain secondary structure through hydrogen bonding. If this hypothesis is correct, replacement of glutamine by larger residues, which would not easily accommodate a water molecule, would be expected to significantly affect nucleotide binding. This was observed with Q214H in the present studies and in previous studies with Q214L (*4*). In addition to effects on nucleotide binding, the data indicate that Gln214 of hTS is involved in the ligand-

induced conformational change, either directly or as a consequence of nonproductive binding of the nucleotide. All mutant proteins examined exhibited a significant decrease in the equilibrium constant for isomerization of enzyme−substrate complexes to the closed form. Furthermore, the mutant enzymes exhibited a slow isomerization after binding CB3717 that was not observed for Q214. The data suggest that Gln214 is located at a structurally critical region of the enzyme.

On the basis of kinetic and thermodynamic constants for nucleotide and CH_2H_4folate binding to hTS, a detailed kinetic mechanism for TMP synthesis for hTS can be constructed (Figure 4). Comparison of the kinetic mechanisms for hTS and ecTS (*14*) revealed that differences occur in nucleotide binding. Interestingly, hTS exhibited a similar affinity for dUMP and FdUMP (Table 1), while the affinity of ecTS was 2-fold lower for FdUMP than dUMP (*14*, *21*). The affinity of hTS was 2-fold higher than that of ecTS for TMP. The k_{chem} of hTS is approximately 2-fold slower compared to that of ecTS. Values of k_{chem} for hTS and ecTS are similar to their respective k_{cat} values at 20 °C, indicating that the chemical steps are rate-limiting for steady-state turnover.

The predicted structures of hTS and ecTS are very similar on the basis of nucleotide sequence (*22*); yet, the crystal structures of the enzymes differ at the active site, as described above (*16*). One concern regarding the reported differences in the structures of unliganded ecTS and hTS is that the crystal structure of hTS may not reflect the solution structure. The data presented herein provide evidence that the enzymes differ in the stability of the closed form of the enzyme−substrate complex, suggesting that they exhibit conformational differences. They also differ in the isomerization induced by binding of the folate inhibitor, CB3717. This raises the concern that inhibitors targeted at hTS that are designed from structures of bacterial TSs may not be optimal.

REFERENCES

1. Dev, I. K., Dallas, W. S., Ferone, R., Hanlon, M., McKee, D. D., and Yates, B. B. (1994) *J. Biol. Chem. 269*, 1873−1882.
2. Jones, T. R., Webber, S. E., Varney, M. D., Reddy, M. R., Lewis, K. K., Kathardekar, V., Mazdiyasni, H., Deal, J., Nguyen, D., Welsh, K. M., Webber, S., Johnston, A., Matthews, D. A., Smith, W. W., Janson, C. A., Bacquet, R. J., Howland, E. F., Booth, C. L., Herrmann, S. M., Ward, R. W., White, J., Bartlett, C. A., and Morse, C. A. (1997) *J. Med. Chem. 40*, 677−683.
3. Carreras, C. W., and Santi, D. V. (1995) *Annu. Rev. Biochem. 64*, 721−762. Dev, I. K., Yates, B. B., Leong, J., and Dallas, W. S. (1988) *Proc. Natl. Acad. Sci. U.S.A. 85*, 1472−1476.
4. Steadman, D. J., Zhao, P.-S., Spencer, H. T., Dunlap, R. B., and Berger, S. H. (1998) *Biochemistry 37*, 7089−7095.
5. Zapf, J. W., Zhao, P.-S., Steadman, D. J., and Berger, S. H. *Biochem. Pharmacol*. (in press).
6. Tong, Y., Liu-Chen, X., Ercikan-Abali, E., Capiaux, G. M., Zhao, S.-C., Banerjee, D., and Bertino, J. R. (1998) *J. Biol. Chem. 273*, 11611−11618.
7. Matthews, D. A., Appelt, K., and Oatley, S. J. (1989) *J. Mol. Biol. 205*, 449−454.
8. Montfort, W. R., Perry, K. M., Fauman, E. B., Finer-Moore, J. S., Maley, G. F., Hardy, L., Maley, F., and Stroud, R. M. (1990) *Biochemistry 29*, 6964−6977.
9. Matthews, D. A., Villafranca, J. E., Janson, C. A., Smith, W. W., Welsh, K., and Freer, S. (1990) *J. Mol. Biol. 214*, 937−948.
10. Finer-Moore, J. S., Liu, L., Schafmeister, C. E., Birdsall, D. L., Mau, T., Santi, D. V., and Stroud, R. M. (1996) *Biochemistry 35*, 5125−5136.
11. Dunlap, R. B., Harding, N. G. L., and Huennekens, F. M. (1971) *Biochemistry 10*, 88−97.
12. Wahba, A. J., and Friedkin, M. (1961) *J. Biol. Chem. 236*, PC11−PC12.
13. Ellis, K. J., and Morrison, J. F. (1982) *Methods Enzymol. 87*, 405−426.
14. Spencer, H. T., Villafranca J. E., and Appleman, J. R. (1997) *Biochemistry 36*, 4212−4222.
15. Mittelstaedt, D. M., and Schimerlik, M. I. (1986) *Arch. Biochem. Biophys. 245*, 417−425.
16. Schiffer, C. A., Clifton, I. J., Davisson, V. J., Santi, D. V., and Stroud, R. M. (1995) *Biochemistry 34*, 16279−16287.
17. Kamb, A., Finer-Moore, J. S., and Stroud, R. M. (1992) *Biochemistry 31*, 12876−12884.
18. Hughey, C. T., Barbour, K. W., Berger, F. G., and Berger, S. H. (1993) *Mol. Pharmacol. 44*, 316−323.
19. Chothia, C. (1976) *J. Mol. Biol. 105*, 1−14.
20. Howell, E. E., Villafranca, J. E., Warren, M. S., Oatley, S. J., and Kraut, J. (1986) *Science 231*, 1123−1128.
21. Weir, M. S., and Dunlap, R. B. (1994) *Nucleosides Nucleotides 13*, 275−291.
22. Perry, K. M., Fauman, E. B., Finer-Moore, J. S., Montfort, W. R., Maley, G. F., Maley, F., and Stroud, R. M. (1990) *Proteins 8*, 315−333.

BI982910N